Article:

Alsaif, A, Bernal, SA orcid.org/0000-0002-9647-3106, Guadagnini, M et al. (1 more author) (2019) Freeze-Thaw Resistance of Steel Fibre Reinforced Rubberised Concrete. Construction and Building Materials, 195. pp. 450-458. ISSN 0950-0618

https://doi.org/10.1016/j.conbuildmat.2018.11.103

Freeze-Thaw Resistance of Steel Fibre Reinforced Rubberised Concrete

Abdulaziz Alsaif,[a,b*], Susan A. Bernal[c,d], Maurizio Guadagnini[a]
Kypros Pilakoutas[a]

[a]Department of Civil and Structural Engineering, The University of Sheffield, Sir Frederick Mappin Building, Mappin Street, Sheffield, S1 3JD, UK.

[b]Department of Civil Engineering, King Saud University, P. O. Box 800, Riyadh 11421, Saudi Arabia.

[c]Department of Materials Science and Engineering, The University of Sheffield, Sir Robert Hadfield Building, Mappin Street, Sheffield, S1 3JD, UK

[d]School of Civil Engineering, University of Leeds, Woodhouse Lane, Leeds, LS2 9JT, UK

[*] Corresponding author: email: asaalsaif1@sheffield.ac.uk; Tel: +44 (0) 114 222 5729,
Fax: +44 (0) 114 2225700

Abstract

This study evaluates the freeze-thaw performance of steel fibre reinforced rubberised concretes (SFRRuC) engineered for flexible concrete pavements. The effect of large volumes of fine and coarse rubber particles (i.e. 30% and 60% volumetric replacement of natural aggregates) is determined for concretes reinforced with 40 kg/m^3 of a blend of manufactured steel fibres and recycled tyre steel fibres. The freeze-thaw performance is assessed through surface scaling, internal damage, residual compressive strength and flexural behaviour. The results show that SFRRuC are able to withstand 56 freeze-thaw cycles with acceptable scaling and without presenting internal damage or degradation in mechanical performance. This indicates that SFRRuC can perform well under extreme freeze-thaw conditions and can be used to construct long-lasting flexible pavements as a sustainable alternative to asphalt concretes.

Keywords: Freeze-thaw; Frost resistance; Rubberised concrete; Steel fibre concrete; Flexible pavements.

1 Introduction

The use of concrete pavement slabs in regions experiencing severe freeze-thaw cycles is challenging, as concretes used for this application must withstand harsh environmental conditions during their service-life. One of the main factors compromising the durability of concrete pavements in such conditions is that drastic changes in temperature produce extra internal stresses causing concrete deterioration [1, 2]. Ice lenses can also form beneath the concrete surface as a result of uneven frost action on the subgrade and can potentially create unsupported regions in the pavement structure and cause additional flexural stresses [3]. Furthermore, de-icing salts, which are used to melt ice and snow, contain high volumes of sodium and/or magnesium chloride and can induce corrosion of the steel reinforcement and surface spalling [4, 5]. Hence, it is required to design concretes that can meet the mechanical strength requirements for paving, with the ability to withstand aggressive in-service conditions such as chlorides attack and freeze-thaw.

According to the European Tyre Recycling Association (ETRA) [6], each year in the 28 European member states and Norway around 300 million post-consumer tyres are discarded as waste. Much of these end up in landfills or are incinerated, despite the fact that they contain high performance constituent materials. According to ETRA [6], the composition of car tyres on the European Union market (by weight) are 48% rubber, 22% carbon black, 15% metal, 5% textile, and 10% others. Strict environmental protocols have been considered in most developed countries to control the disposal of waste tyres and the European Directive 1991/31/EC [7] has forbidden the land filling of whole post-consumer tyres since 2003 and shredded tyres since 2006 [8-10]. The European Directive 2008/98/EC [11] has provided a disposal hierarchy to encourage the management of post-consumer tyres that places reuse and recycling above incineration. A possible waste management solution is to find use for the post-consumer tyre materials in the construction industry. This improves sustainability by preventing environmental pollution as well as saving natural aggregate from depletion, and it is economically viable as some of the costly conventional materials (e.g. steel fibres) can be saved.

During the last three decades, rubber aggregates have been used in asphalt-rubber mixtures for pavement applications [12]. It has been noted that the use of rubber helps to reduce noise and increase resistance to temperature variation and freeze-thaw action, thus lowering maintenance costs and enhancing service life [13, 14]. The use of rubber aggregates as a partial substitution of natural aggregates in concrete has also been investigated by several researchers [8, 15-17]. It has been demonstrated that, compared to conventional concrete, rubberised concrete (RuC) has larger deformability [15, 18], lower density [19-21], and higher sound absorption, skid and impact resistance as well as enhanced electrical and thermal insulation [10, 22-24]. Conversely, RuC suffers from increased air content as well as reduced workability, strength and stiffness [8, 25, 26]. As a result, RuC is rarely used in structural applications.

The durability properties of RuC are also not well understood. Few studies have assessed the freeze-thaw resistance of RuC and most focused on the resistance of RuC containing crumb rubber only [1, 2, 27-30]. Savas et al. [30] investigated the freeze-thaw resistance of RuC containing different amounts of crumb rubber. They observed that RuC mixes with replacement ratios of 10% and 15% by weight of cement (2–6 mm in size) exhibited durability factors (DFs) higher than the minimum 60% after 300 freeze-thaw cycles specified by ASTM C666/C666M-15 [31], whereas mixes with 20% and 30% could not meet the minimum DF recommended. Similarly, Kardos and Durham [32] assessed the rapid freeze-thaw resistance of plain concrete and RuC mixes with up to 50% sand replacement by volume. The authors found that RuC containing 10% crumb rubber exhibited the highest DF followed by the 20% RuC while the plain concrete and 30% RuC, showed comparable DFs. The 40% RuC and 50% RuC failed to withstand freeze-thaw action after 300 cycles as their DFs fell below 60%. Richardson et al. [28, 29], on the other hand, indicated that the addition of 0.6% by weight of crumb rubber with size smaller than 0.5 mm provided significant freeze-thaw protection in concrete.

Deterioration of concrete subjected to repeated freeze-thaw actions occur due to the formation of micro ice bodies within the concrete pores, which expand up to 9% compared to the volume of water [33, 34]. If the concrete paste becomes critically saturated and there is no space for this volume expansion, hydraulic pressures and tensile stresses can be generated in the pores, contributing to pore enlargement [35]. Consequently, the enlarged pores can be filled with water from the environment due to water uptake phenomena, causing larger tensile stress when frozen again and eventually leading to deterioration. Hence, the pore structure governs the rate and level of damage caused by freeze-thaw. More interconnected and larger pores are expected to lead to more water uptake and damage. The freeze-thaw resistance of concrete can be improved by providing air-entraining agents to create empty and closely spaced bubbles, which act as receiver of the excess water, thus relieving the pressure created in the concrete due to ice formation. In full saturation conditions, however, "the hydraulic pressure theory" is not applicable since non-frozen water cannot find a way to escape [36]. It is believed that crumb rubber particles can promote the formation of pores of similar quality to those created by air-entraining agents [28, 37]. Khalo et al. [25] attributed the entrapment of air to the hydrophobic nature and rough surfaces of rubber particles, which entrap air during the mixing process. Hence, it is evident that the amount and size of rubber particles incorporated play a major role in the RuC freeze-thaw resistance, but there appears to be a limit to the replacement ratio that can lead to beneficial results. It has been reported for rubberised mortars and concretes that the amount of rubber replacement should be limited to a maximum of 10% [2] or 30% [32] by volume of fine aggregate in order to obtain acceptable durability.

In a recent study, the authors [38] demonstrated that the inclusion of fibres in RuC with high volumes of rubber (e.g. 30% or 60%) promote the development of SFRRuC with enhanced flexibility and ductility characteristics and flexural strengths that comply with the specifications defined in pavement design EN 13877-1 [39]. It has also been identified [40] that the substitution of natural aggregate by rubber particles increases the permeability of SFRRuC (i.e. volume of permeable voids and sorptivity) as rubber content increases. However, this increment is minor and the permeability properties of these concretes lie within the range of highly durable concretes. Furthermore, SFRRuC exhibit very high resistance to chloride permeability when assessed under accelerated wet-dry cycles [40]. The combination of such properties makes SFRRuC mixes ideal candidates for flexible concrete pavements. However, the effect of large volume of rubber on freeze-thaw resistance needs to be addressed. Due to the weak bond between cementitious materials and rubber particles [25, 26], micro-cracks forming in RuCs might propagate locally at a fast rate, making these materials more prone to damage. However, the authors hypothesised that this issue would be greatly mitigated by the inclusion of fibres in RuC as fibres tend to bridge micro-cracks and resist their opening. Hence, this study aims to examine the influence of freeze-thaw on the performance of SFRRuC under accelerated conditions. Performance is assessed through visual inspection of the specimens, mass loss, coefficient of thermal expansion (CTE), changes in relative dynamic modulus of elasticity (RDM), and residual mechanical properties including compressive strength, flexural strength, flexural modulus of elasticity and toughness.

2 Experimental Programme

2.1 Materials and concrete mix designs

2.1.1 Materials

Concrete mixtures were produced using a ternary blend of Portland lime cement type CEM II 52.5N, with silica fume (SF) and pulverised fuel ash (PFA) as cement replacements (10% by weight for each). Two types of high range water-reducing admixtures were used: a) polycarboxylate polymer plasticiser and b) superplasticiser

Natural river sand with particle size of 0/5 mm and specific gravity (SG) of 2.64 was used as fine aggregate (FA), while natural river gravel with particle sizes of 5/10 mm and 10/20 mm and a SG of 2.65 was employed as coarse aggregate (CA). Rubber aggregates used in this experimental study were recovered mechanically from post-consumer tyres. The fine rubber (FR) particles were supplied in three different sizes, 0/0.5 mm, 0.5/2 mm and 2/6 mm, and were used to replace 22.2%, 33.4%, 44.4% of FA volume, respectively. The course rubber (CR) particles were provided in two sizes, 5/10 mm and 10/20 mm, and were used to replace the CA in equal amounts. The specific gravity of 0.8, determined by the authors [38], was employed to calculate the volume of rubber particles. Fig. 1 shows the particle size distribution of all aggregates used in this study, obtained according to ASTM-C136 [41].

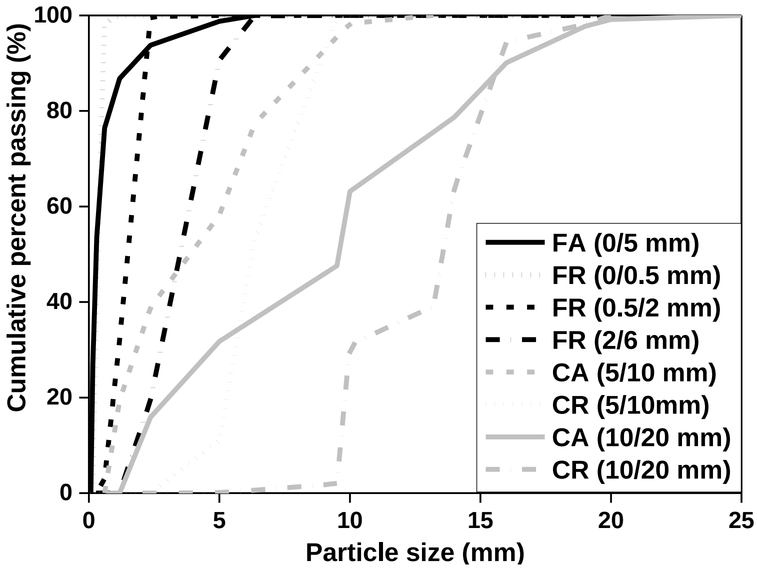

Fig. 1 Particle size distributions

2.1.2 Concrete mix designs

Four different concrete mixes were prepared in this study including a plain concrete mix, a steel fibre reinforced concrete (SFRC) mix, and two SFRC rubberised concrete (SFRRuC) mixes, in which rubber aggregates were used as partial replacement for both FA and CA with 30% or 60% by volume. The amount of steel fibres added in the SFRC and SFRRuC mixes was 40 kg/m^3, as used in structural concrete, using equal amount of: a) crimped type manufactured steel fibres (MSF) with lengths of 55 mm and diameters of 0.8, and b) recycled tyre steel fibres (RTSF) with lengths between 15-45 mm (>60% by mass) and diameters <0.3 mm. Further details about the fibres characteristics are reported in [38, 42].

A mix ID was adopted for easy reference. It contains a number and a letter, where the number can be 0, 30 or 60, denoting the volumetric percentages of rubber aggregates used as partial replacement of natural aggregates, while the letter can be either P or BF (Plain or Blend of Fibres, respectively), referring to the absence or presence of the steel fibre reinforcement in the concrete mix. Table 1 shows the mixes IDs and variables.

Table 1 Mixes IDs and variables

Mix ID	0P	0BF	30BF	60BF
FR replacing FA by volume (%)	0	0	30	60
CR replacing CA by volume (%)	0	0	30	60
Amount of MSF (kg/m^3)	0	20	20	20
Amount of RTSF (kg/m^3)	0	20	20	20

All concretes assessed in this study were designed with 340 kg/m^3 of Portland cement, 42.5 kg/m^3 of SF, 42.5 kg/m^3 of PFA , 820 kg/m^3 of FA, 1001 kg/m^3 of CA, 150 l/m^3 of tap water (water /cement = 0.35), with 2.5 l/m^3 of plasticiser and 5.1 l/m^3 of superplasticiser. All mix design parameters were kept constant in this study except from the aggregates volume (see section 2.1.1). This study targeted slump of class S3 according to EN 206 [43] or higher (≥ 90 mm), therefore, the amount of plasticiser was also increased to 3.25 l/m^3 for 30BF mix and to 4.25 l/m^3 for 60BF mix to attain the targeted slump. The adopted concrete mix design was selected based on the outcomes of a previous study [21] evaluating RuC, in which it was identified that similar large volumes of aggregate replacements do not induce excessive degradation in fresh properties compared with reference concretes without rubber.

2.1.3 Mixing, casting and curing procedure

The production of the concrete mixes started with dry mixing natural and rubber aggregates for 30 s using a pan mixer. Half of the total amount of water was then introduced to the mixer, and the materials were mixed for another 1 min. Subsequently, mixing was halted for 3 min, to allow aggregates to gain saturation, and the cementitious materials were added. After that, mixing was continued for 3 min during which the remaining water and chemical admixtures were gradually added. Finally, the steel fibres were manually integrated, and mixing was continued for another 3 min.

Prior to casting, the concrete fresh properties including slump, air content and unit weight were assessed based on methods described in EN 12350-2 [44], EN 12350-7 [45], and EN 12350-6 [46], respectively. Table 2 summarises the fresh properties of the concrete mixes. The results show that the inclusion of rubber particles in the fresh concrete mixes reduces the slump and unit weight, and increases the air content.

Table 2 Fresh properties of the tested concrete mixes

Mix ID	0P	0BF	30BF	60BF
Slump (mm)	235	200	155	110
Air content (%)	1.7	1.3	2.3	2.9
Unit weight (kg/m^3)	2401	2425	2175	1865

Concrete was cast in the moulds using two layers of casting (according to EN 12390-2) [47] and was vibrated on a shaking table (25s per layer). The specimens were then cured in the moulds for 48 h with wet hessian and sealed with plastic. Subsequently, all specimens were stored in a mist room at a temperature of 21 ℃ $\pm$ 2 and relative humidity of 95 $\pm$ 5% for 10 months. This curing age was selected considering that in countries experiencing severe winters, concrete casting on-site typically takes place in spring (or summer) and therefore it is most likely that the first freeze-thaw will be experienced within 10 months of age.

Four cubes and three prisms per mix were removed from the mist room, marked as 'F-T' and subjected to freeze-thaw conditions, while a similar number of specimens was kept as 'control' in the mist room. The compressive strength and flexural behaviour of all 'F-T' and 'control' specimens were evaluated at the end of the freeze-thaw conditioning period. Two prisms per mix were used to assess the coefficient of thermal expansion (CTE) as described in section 3.2.

2.2 Test set-up and instrumentation

2.2.1 Freeze-thaw testing

The freeze-thaw resistance of concrete cubes and prisms was assessed based on: (i) visual analysis in terms of damage caused by freeze-thaw action, (ii) mass loss due to cubes scaling following the recommendation of PD CEN/TS 12390-9 [48], (iii) beam tests according to PD CEN/TR15177 [49] to assess the internal damage of concrete prisms through the evaluation of their RDMs using the measurements obtained from ultrasonic pulse transit time (UPTT), and (iv) residual compressive strength and flexural behaviour.

The concrete specimens were placed in stainless steel containers and were fully immersed in a 3% NaCl solution. The containers were then placed into a chamber that was programmed to apply continuous cycles of freeze and thaw with temperature ranging from -15 °C to 20 °C and controlled through a thermocouple embedded in the centre of a concrete cube. Fig. 2 shows the experimental temperature profile compared with the desired temperature profile specified in PD CEN/TS 12390-9 [48].

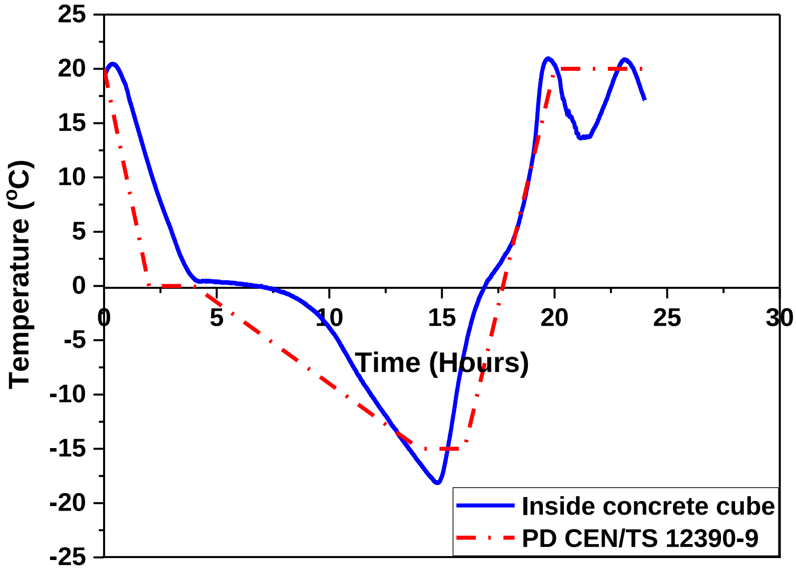

Fig. 2 Temperature profile measured in the centre of a concrete cube using a thermocouple, compared with that of PD CEN/TS 12390-9 [48]

The mass loss and UPTT were determined after 7, 14, 28, 42 and 56 freeze-thaw cycles. At each of these defined cycles, during the thawing phase, the concrete cubes and prisms were removed and first visually examined in terms of surface damage. The cubes were then thoroughly brushed to remove any loose parts and then weighed. All detached materials were collected, oven dried for 24 hours at 105 °C and weighed to the nearest 0.1g. The percentage of cumulative mass loss after n cycles, was calculated according to Equation (1):

$$\text{Cummulative mass loss } (\%), \text{n} = \frac{\sum_{i=1}^{n} \mathrm{M}_{d,n}}{M_0} \cdot 100 \qquad (1)$$

where, $M_{d,n}$ is the mass of the oven dried scaled material collected after cycle n, and M_0 is the initial mass of specimens after curing and before testing.

Similarly, the concrete prisms were thoroughly brushed, surface dried, and were then fitted with two transducers on the two opposite sides of the prisms to measure the UPTT. The transducers were pressed against the concrete surfaces, using the same pressure each time, until a constant minimum value was achieved. The RDM of elasticity after n cycles, was calculated using Equation (2) below;

$$\mathrm{RDM, n}\ (\%) = \left(\frac{UPTT_0}{UPTT_n}\right)^2 \cdot 100 \quad (2)$$

where $UPTT_0$ is the initial UPTT of the specimen, in μs, while UPTTn is the specimen UPTT after n freeze-thaw cycles, in μs. Cubes and prisms were then returned to the containers with fresh 3% NaCl solution and test was resumed.

2.2.2 Compressive cube tests and flexural tests on prisms

Concrete cubes were tested under uniaxial compressive loading according to EN 12390-3 [50] at a loading rate of 0.4 MPa/s. Concrete prisms were tested under 4-point bending test configuration following the recommendations of the JSCE [51], using an electromechanical testing machine. The net mid-span deflection was recorded by two linear variable differential transformers (LVDTs), placed on an aluminium yoke. The load was applied in displacement control at a constant rate of deflection at the mid-span of the prism of 0.2 mm/min until a deflection of 6 mm.

2.2.3 Coefficient of thermal expansion

The CTE was determined according to the TI-B 101 procedure [52] using two duplicate prisms per mix. The CTE of the rubber particles used in this study was also determined to be approximately 80 x 10^{-6} m/mK, which is 10 times higher than that of the limestone natural aggregates used in this study, and obtained from FDA [53]. Such significant difference in CTE may induce internal stresses during the freeze-thaw cycles.

3 Results and Discussion

3.1 Visual inspection

Fig. 3 shows the appearance of the tested specimens before and after completing 56 cycles of freeze-thaw action. Surface scaling and concrete pop-outs are the two signs of deterioration that are observed in all tested specimens. Surface scaling (i.e. delamination) is expected to develop when internal stresses exceed the tensile or shear strength of the surface layer, whilst the build-up of pressure around the coarse aggregate particles can cause the concrete between the particles and the nearest concrete face to pop-outs [54].

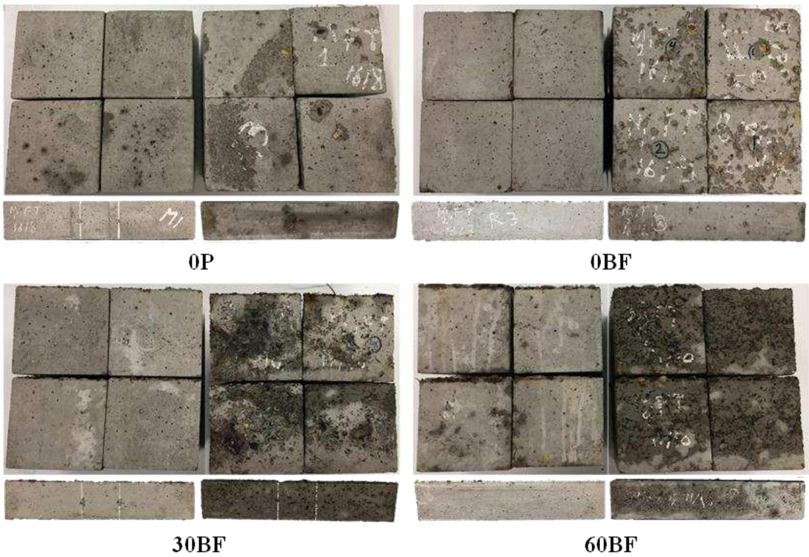

Fig. 3 Specimens appearance before (left) and after (right) completing 56 cycles of freeze-thaw action

ASTM C672/C672M – 12 [55] specifies a visual rating category depending on the severity of surface scaling, as shown in Table 3. Based on the appearance of the concretes after exposure (Fig. 3), concretes without rubber aggregates (i.e. 0P and 0BF) are rated 3, while SFRRuC specimens (i.e. 30BF and 60BF) are rated 4. The amount of concrete scaling and mortar coming off at the end of the freeze-thaw cycles is higher in rubberised concrete. This is a likely consequence of the higher volume of permeable voids (VPV) identified in SFRRuC (see Fig. 4 [40]), and the resulting increase in water uptake of the samples during testing compared to specimens without rubber aggregates. It has been reported [56] that the connectivity of pores is higher at the surface of the concrete specimens and typically increases at higher freeze-thaw cycles. Therefore, concretes with higher permeability are expected to suffer more severe damage. Despite the fact that the SFRRuC specimens show moderate to severe scaling, they withstood 56 freeze-thaw cycles without severe damage.

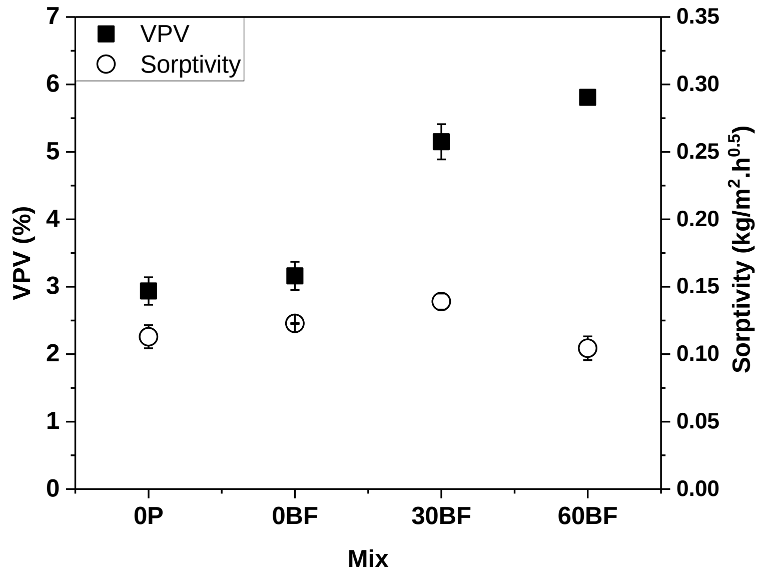

Fig. 4 VPV (left) and sorptivity (right) of all tested concretes [40]

Table 3 Surface scaling rating adapted from ASTM C672/C672M – 12 [55]

Rating	Condition of surface
0	No scaling
1	Very slight scaling (3 mm [1/8 in.] depth max., no coarse aggregate visible
2	Slight to moderate scaling
3	Moderate scaling (some coarse aggregate visible)
4	Moderate to severe scaling
5	Sever scaling (coarse aggregate visible over entire surface)

3.2 Mass of scaled concretes

Fig. 5 shows the mean cumulative mass loss versus the number of freeze-thaw cycles. Error bars represent one standard deviation of four measurements. It is evident that 0P specimens exhibit minimal mass loss throughout the test, while 0BF and 60BF specimens show similar mass loss behaviour, which is higher than 0P. The SFRRuC specimens with 30% rubber replacement, 30BF, display the highest rate of mass loss, especially after 14 freeze-thaw cycles. A previous study by the authors [40] on the transport properties of the same four concrete mixes shows that 30BF specimens present the highest sorptivity values (see Fig. 4). The higher sorptivity for the 30BF specimens was attributed to the large amount of fine pores which facilitated water uptake and caused these specimens to be more prone to damage due to freeze-thaw cycles. On the other hand, owing to the high amount of large coarse rubber particles and the non-sorptive nature of rubber, a reduction in sorptivity was observed in the 60BF specimens.

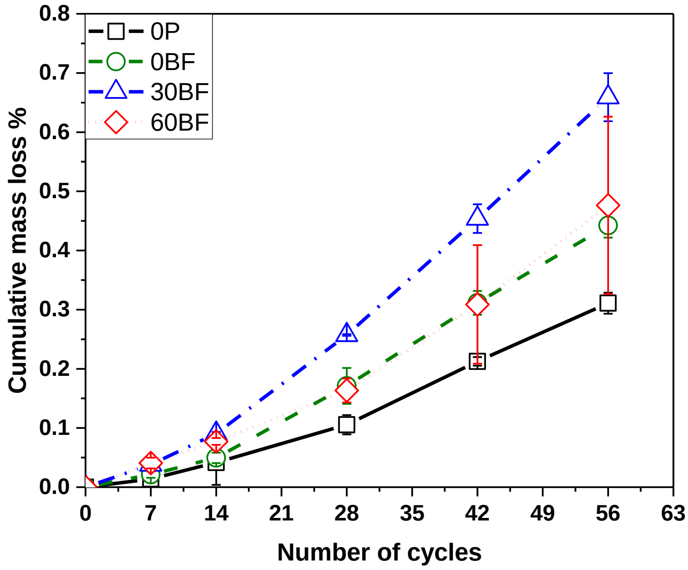

Fig. 5 Cumulative mass loss as a function of freeze-thaw cycles

For all concrete mixes, the ratios between the masses of scaled materials after completing 56 freeze-thaw cycles (M_{56}) to that after 28 cycles (M_{28}) are lower than two, and the M_{56} are less than 1.0 kg/m^2 (see Table 4). Hence, they all fall under the acceptable resistance category, as specified by the Swedish standard SS 13 72 44 ED [57]. Consequently, this study contradicts previous work [2, 32] and shows that when using fibres, the amount of rubber aggregates can be significantly increased (up to 60%) without compromising durability.

The high resistance to freeze-thaw exhibited by the tested concretes can not be attributed to differences in thermal properties as minimal changes in the coefficient of thermal expansion (CTE) were obtained (see Table 5). This indicates that rubber aggregates may counteract the freeze-thaw effect even in highly porous concretes due to their low stiffness, which offers less resistance to expansion. It should also be noted that the addition of rubber increases air entrainment (see VPV in Fig. 4), as found in [40], which can also create a pressure release system for freeze-thaw phenomena [58]. Furthermore, rubber particles, with their excellent damping characteristic [20, 59], may contribute somehow in balancing the internal stresses and act like absorbers for the temperature and freeze-thaw induced stresses and deformations [4]. The fibre blends also participate by bridging and controlling cracks.

Table 4 Mass loss results for all concrete mixes

Mix	M_{56}/M_{28}	Mass of scaled materials after 56 cycles, M_{56} (kg/m^2)
0P	1.5	0.5
0BF	1.1	0.6
30BF	1.2	0.9
60BF	1.9	0.7

Table 5 Coefficient of thermal expansions obtained for all concrete mixes

Mix	Coefficient of thermal expansion × 10^{-6} m/mk
0P	10.3-12.2
0BF	10.3-11
30BF	9.0-11.6
60BF	9.7-12.9

3.3 Effect of freeze-thaw on mechanical performance

3.3.1 Compressive strength

Table 6 summarises the average compressive strength and standard deviation (in brackets) derived from testing four specimens for each of the examined concretes. As expected, the addition of blended fibres enhances the compressive strength of control specimen 0BF by 7% with respect to 0P. The partial replacement of natural aggregates with rubber particles, however, considerably reduces the compressive strength reporting an average reduction of 58% for 30BF and 88% for 60BF compared to 0BF. The two mechanisms responsible for such degradation in compressive strength are: (i) the lower stiffness and higher Poisson ratio of rubber compared to natural aggregates, and (ii) bond defects between rubber particles and matrix [25, 26]. Further discussions regarding the compressive strength reduction mechanism in SFRRuC are reported in [38], where similar results were obtained.

Table 6 Average compressive strength results of all concrete mixes

Mix	Compressive strength (MPa)		
	Control	F-T	Change on control (%)
0P	111 (3.8)	108 (3.8)	-3
0BF	118 (0.9)	110 (7.7)	-7
30BF	50 (4.0)	40 (5.3)	-20
60BF	14 (3.0)	12 (2.0)	-14

After 56 cycles of freeze-thaw (F-T), all concrete specimens exhibit minor compressive strength loss compared to the control specimens of the same mixes. The slight reduction in the compressive strength indicates that the freeze-thaw action has affected mostly the surface of the concrete, without compromising its internal integrity.

A good correlation is identified between the compressive strength and cumulative mass loss for all concrete specimens at the end of the 56 cycles (see Fig. 6). The 30BF specimens show the highest amount of cumulative mass loss, 0.66%, and compressive strength loss, 20%, which were most likely caused by the higher sorptivity of this mix (see Fig. 4).

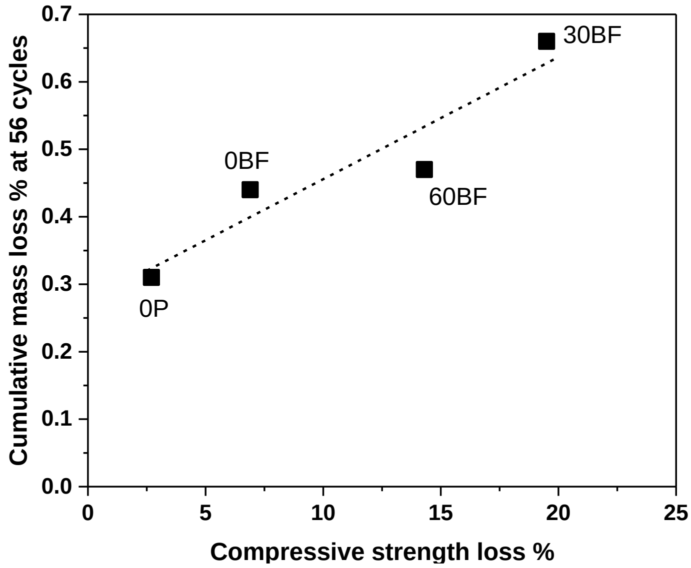

Fig. 6 Correlation between the percentage of cumulative mass loss and compressive strength loss at the end of 56 freeze-thaw cycles

3.3.2 Flexural strength

Table 7 summarises the average values of flexural strength, modulus of elasticity and toughness of the control and F-T specimens as obtained from testing three specimens per mix. Values in brackets represent standard deviation.

Table 7 Average flexural strength, modulus of elasticity and toughness factor

Mix		0P	0BF	30BF	60BF
Flexural strength (MPa)	Control	8.1 (1.1)	9.4 (1.0)	6.1 (1.0)	3.7 (0.6)
	F-T	8.5 (1.3)	9.1 (0.5)	4.9 (0.8)	3.9 (0.6)
	Change on control (%)	5	-3	-20	5
Flexural modulus of elasticity (GPa)	Control	48 (2.2)	46 (0.1)	26 (0.5)	9.3 (1.0)
	F-T	47 (4.3)	44 (1.5)	25 (0.7)	8.8 (1.1)
	Change on control (%)	-3	-3	-3	-5
Flexural toughness factor (MPa)	Control	-	5.9 (0.3)	5.2 (0.9)	3.2 (0.5)
	F-T	-	5.2 (0.9)	3.8 (0.7)	3.4 (0.3)
	Change on control (%)	-	-12	-27	6

Table 7 shows that the addition of blended fibres enhances the flexural strength of 0BF control specimens by 5%, compared to 0P. On the other hand, the replacement of 30% and 60% of natural aggregates with rubber particles, as expected, reduces the flexural strength by 35% and 60% respectively, compared to 0BF. It should be noted that the presence of steel fibres in SFRRuC mixes effectively mitigates the rate of reduction in flexural strength, compared to that in compressive strength, due to the ability of the fibres to control micro-cracking, as discussed in Alsaif et al. [38].

After completing 56 cycles of freeze-thaw action, the concretes 0P, 0BF and 60BF show comparable flexural strength values to those of control specimens of the same mixes with small differences within one standard deviation. The flexural strength of the 30BF specimens after 56 cycles of freeze thaw action, however, is 20% below that of the control specimens of the same mix, which is consistent with the reduction in compressive strength reported in Table 6. As mentioned earlier, the high sorptivity in the 30BF mix [40] may have caused this reduction in strength. Nevertheless, all SFRRuC specimens studied here (both F-T and control) satisfy the flexural strength requirements specified in pavement design EN 13877-1[39].

3.3.3 Flexural modulus of elasticity

The elastic beam theory was adopted in this study to determine the secant modulus of elasticity of the load-deflection curves considering the region from 0 to 40% of the peak load. As shown in Table 7, the addition of steel fibres in conventional concrete specimens, 0BF, marginally reduces the modulus of elasticity compared to 0P specimens. This reduction was not anticipated as the addition of fibres was expected to slightly increase the modulus of elasticity of the composite due to their high stiffness, but may be explained by the increased volume of permeable voids, as discussed in [40]. The substantial decrease in the modulus of elasticity, however, for the SFRRuC specimens (48% for 30BF and 80% for 60BF) was expected due to the lower stiffness of the rubber aggregates, compared to the replaced natural aggregates [38]. After freeze-thaw action, minor reductions (3-5%) in the modulus of elasticity were recorded. The RDM was also investigated and it is discussed in the following section.

3.3.3.1 Relative dynamic modulus of elasticity

Fig. 7 shows the mean RDM values as a function of the number of freeze-thaw cycles applied. Error bars represent one standard deviation of three measurements. It is worth mentioning that, during the periodical measurements, occasionally UPTT values went down due to difficulties of making contact with the sides of the concrete prism as these were severely roughened due to scaling. In general, the RDM values decrease with increasing number of freeze-thaw cycles. This is expected due to the typical increase in water uptake (capillary pores imbibe water) and, hence the UPTT values. It is also evident from Fig. 7 that the rate of reduction in RDM values increases with the rubber content. This may indicate some loss in the bond between the rubber and cementitious materials [1], possibly due to the weak adhesion in the interfacial transition zone (ITZ). As all specimens survived 56 freeze-thaw cycles and their RDM values are above the threshold value of 80% defined by RILEM 2004 [60], all concrete mixes can be considered to be durable.

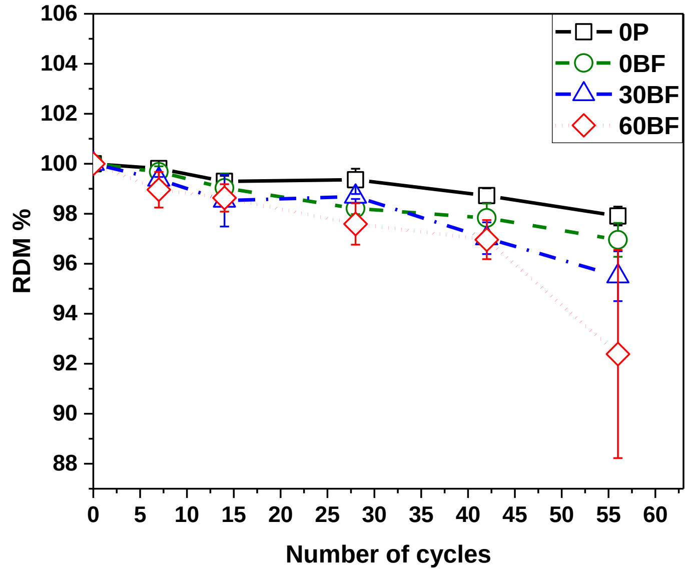

Fig. 7 Change in relative dynamic modulus during freeze/thaw cycles

3.3.4 Load-deflection curve and flexural toughness factor

Fig. 8 shows the average (of 3 prisms) stress-deflection curves. While the plain concrete specimens, 0P, failed suddenly after reaching the peak stress, highlighting the brittleness of plain concrete in tension, 0BF, 30BF and 60BF specimens continued sustaining further flexural stresses even after first crack. This is mainly due to the contribution of fibres in dissipating energy through their pull-out mechanism as well as in bridging cracks and resisting their opening [38]. Rubber particles also participated partially in enhancing the post-peak behaviour by absorbing some of the energy during loading and undergoing large deformation as identified by the authors in a previous study [38].

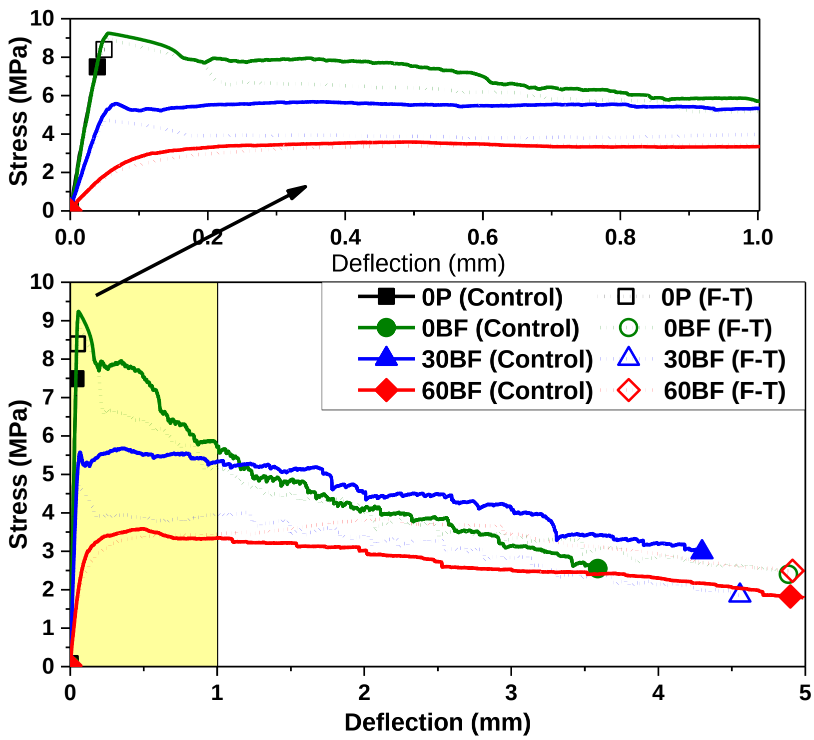

Fig. 8 Average stress versus deflection curves for all concrete mixes

To further examine the effect of freeze-thaw action on the flexural behaviour of SFRC and SFRRuC, the flexural toughness factors were obtained (see Table 7) according to JSCE [51]. The toughness factor of the plain concrete mix, 0P, is not included as its post-peak energy absorption behaviour is negligible. The area under the load-deflection curve is computed up to a deflection of $\delta_f = 2$ mm and the flexural toughness factor is calculated according to Equation (3).

$$\text{Flexural toughness factor (MPa)} = \frac{Area\ under\ the\ curve \cdot L}{2 \cdot b \cdot h^2} \quad (3)$$

where L is the span length, in mm, b is the width of the specimen, in mm, h is the high of the specimen, in mm.

The toughness factor is found to decrease with increasing rubber content mainly due to the large reduction in flexural strength. After freeze-thaw action, the toughness factor decreases by 12% for 0BF and 27% for 30BF while it increases by 6% for 60BF. Overall, F-T action did not have a major impact on flexural performance, except for 30BF specimens due to their higher sorptivity (see Fig. 4). This is mainly attributed to the presence of fibres which are more effective in enhancing flexural behaviour through mechanisms (crack bridging) that are not significantly affected by freeze-thaw.

3.4 General discussion on practical use

Previous research by the authors [38] showed that optimised flexible SFRRuC mixes were able to attain high ductility and flexibility, and achieve workability properties and flexural strengths that meet the specifications defined in pavement design [39]. It has also been identified in a subsequent research study [40] that the durability and permeability properties of these flexible SFRRuC mixes lie within the range of highly durable concrete based on commonly accepted "durability indicators" [57, 60-62]. In this article, the authors demonstrate the ability of these SFRRuC mixes to withstand 56 freeze-thaw cycles with acceptable scaling and without presenting internal damage or degradation in mechanical performance. Furthermore, the inclusion of a large amounts of waste tyre rubber leads to the development of flexible SFRRuC pavements with stiffness values similar to those of flexible asphalt pavements, i.e. around 8 GPa [7]. Hence, these flexible SFRRuC are expected to accommodate subgrade induced movements and settlements arising from poor compaction during construction or temperature variations, including freeze-thaw. The body of this work shows that SFRRuC, which can be manufactured using conventional mixing techniques, is a promising solution for building sustainable road pavements."

4 Conclusion

This study assessed the freeze-thaw performance of steel fibre reinforced rubberised concretes (SFRRuC) produced with large contents of waste tyre rubber and reinforced with a blend of manufactured and recycled tyre steel fibres. Based on the experimental results, this study shows that all SFRRuC mixes successfully withstood 56 freeze-thaw cycles without being significantly damaged. The cubes show acceptable scaling resistance according to the Swedish Criteria SS 13 72 44 ED, while the prisms maintain RDMs values above the threshold value for internal damage (80%) specified in RILEM TC 176-IDC. Hence, as hypothesised by the authors, the inclusion of steel fibres in RuC greatly mitigates the negative effects of large volumes of rubber on freeze-thaw resistance.

The presence of steel fibres in SFRRuC mixes significantly reduces the rate of reduction in flexural strength due to the addition of large volumes of rubber, compared to that in compressive strength. All SFRRuC mixes show flexural strengths that satisfy the requirement for pavement design according to EN 13877-1.

Comparable mechanical performance is observed from specimens subjected to freeze-thaw and control specimens kept in the mist room, thus making SFRRuC a potentially sustainable flexible concrete pavement solution capable of adequate freeze-thaw performance. For pavement applications, future studies should investigate the fatigue performance of this novel concrete.

Acknowledgements

The current experimental work was undertaken under the FP7 European funded collaborative project "Anagennisi: Innovative reuse of all tyre components in concrete" (Contract agreement number: 603722). The following companies offered materials and valuable in-kind contribution: Tarmac UK, Twincon Ltd, Aggregate Industries UK and Ltd Sika. Mr Alsaif would like to thank King Saud University and the Ministry of Education (Kingdom of Saudi Arabia) for sponsoring his PhD studies. Dr S.A. Bernal participation in this study has been sponsored by EPSRC through her ECF (EP/R001642/1).

References

[1] K.A. Paine, R. Dhir, R. Moroney, and K. Kopasakis. *Use of crumb rubber to achieve freeze/thaw resisting concrete*. in *Challenges of Concrete Construction: Volume 6, Concrete for Extreme Conditions: Proceedings of the International Conference held at the University of Dundee, Scotland, UK on 9–11 September 2002*. 2002: Thomas Telford Publishing.

[2] İ.B. Topçu and A. Demir. *Durability of rubberized mortar and concrete.* Journal Of Materials In Civil Engineering 2007;19(2):173-178.

[3] A. Vaitkus, J. Gražulytė, E. Skrodenis, and I. Kravcovas. *Design of Frost Resistant Pavement Structure Based on Road Weather Stations (RWSs) Data.* Sustainability 2016;8(12):1328.

[4] O.A. Abaza and Z.S. Hussein. *Flexural Behavior of Steel Fiber-Reinforced Rubberized Concrete.* Journal Of Materials In Civil Engineering 2015;28(1):04015076.

[5] V. Baroghel-Bouny, P. Belin, M. Maultzsch, and D. Henry. *$AgNO_3$ spray tests: advantages, weaknesses, and various applications to quantify chloride ingress into concrete. Part 1: Non-steady-state diffusion tests and exposure to natural conditions.* Materials and Structures 2007;40(8):759-781.

[6] ETRA, *The European Tyre Recycling Association*. 2016, Available at: http://www.etra-eu.org [Last accessed: 02/01/2018].

[7] Council of the European Union, *Council Directive 1999/31/EC of 26 April 1999 on the landfill of waste*. 1999.

[8] N.N. Eldin and A.B. Senouci. *Measurement and prediction of the strength of rubberized concrete.* Cement and Concrete Composites 1994;16(4):287-298.

[9] A. Benazzouk, O. Douzane, K. Mezreb, B. Laidoudi, and M. Queneudec. *Thermal conductivity of cement composites containing rubber waste particles: Experimental study and modelling.* Construction and Building Materials 2008;22(4):573-579.

[10] B.S. Mohammed, K.M.A. Hossain, J.T.E. Swee, G. Wong, and M. Abdullahi. *Properties of crumb rubber hollow concrete block.* Journal Of Cleaner Production 2012;23(1):57-67.

[11] Council of the European Union, *Council Directive 2008/98/EC on waste (Waste Framework Directive)*. 2008.

[12] J.A. Epps, *Uses of recycled rubber tires in highways*. Vol. 198. 1994: Transportation Research Board.

[13] S.N. Amirkhanian and J.L. Burati Jr, *Utilization of waste tires in asphaltic materials. Clemson Univ., SC (United States). Dept. of Civil Engineering. Technical Report;PB-96-203062/XAB,CNN: Contract SPR-554; TRN: 62752193.* 1996.

[14] B. Adhikari, D. De, and S. Maiti. *Reclamation and recycling of waste rubber.* Progress in polymer science 2000;25(7):909-948.

[15] S. Raffoul, R. Garcia, D. Escolano-Margarit, M. Guadagnini, I. Hajirasouliha, and K. Pilakoutas. *Behaviour of unconfined and FRP-confined rubberised concrete in axial compression.* Construction and Building Materials 2017;147:388-397.

[16] F. Hernández-Olivares and G. Barluenga. *Fire performance of recycled rubber-filled high-strength concrete.* Cement And Concrete Research 2004;34(1):109-117.

[17] F. Hernández-Olivares, G. Barluenga, M. Bollati, and B. Witoszek. *Static and dynamic behaviour of recycled tyre rubber-filled concrete.* Cement And Concrete Research 2002;32(10):1587-1596.

[18] A. Alsaif, R. Garcia, M. Guadagnini, and K. Pilakoutas, *Behaviour of FRP-Confined Rubberised Concrete with Internal Recycled Tyre Steel Fibres*, in *High Tech Concrete: Where Technology and Engineering Meet: Proceedings of the 2017 fib Symposium, held in Maastricht, The Netherlands, June 12–14, 2017*, D.A. Hordijk and M. Luković, Editors. 2018, Springer International Publishing: Cham. p. 233-241.

[19] A. Grinys, H. Sivilevičius, D. Pupeikis, and E. Ivanauskas. *Fracture of concrete containing crumb rubber.* Journal of Civil Engineering and Management 2013;19(3):447-455.

[20] F. Liu, W. Zheng, L. Li, W. Feng, and G. Ning. *Mechanical and fatigue performance of rubber concrete.* Construction and Building Materials 2013;47:711-719.

[21] S. Raffoul, R. Garcia, K. Pilakoutas, M. Guadagnini, and N.F. Medina. *Optimisation of rubberised concrete with high rubber content: An experimental investigation.* Construction and Building Materials 2016;124:391-404.

[22] P. Sukontasukkul and C. Chaikaew. *Properties of concrete pedestrian block mixed with crumb rubber.* Construction and Building Materials 2006;20(7):450-457.

[23] T.C. Ling, H.M. Nor, and S.K. Lim. *Using recycled waste tyres in concrete paving blocks.* Proceedings of the ICE - Waste and Resource Management 2010;163(1):37-45.

[24] C.A. Issa and G. Salem. *Utilization of recycled crumb rubber as fine aggregates in concrete mix design.* Construction and Building Materials 2013;42:48-52.

[25] A.R. Khaloo, M. Dehestani, and P. Rahmatabadi. *Mechanical properties of concrete containing a high volume of tire–rubber particles.* Waste management 2008;28(12):2472-2482.

[26] Z. Khatib and F. Bayomy. *Rubberized portland cement concrete.* Journal Of Materials In Civil Engineering 1999;11(3):206-213.

[27] X. Zhu, C. Miao, J. Liu, and J. Hong. *Influence of crumb rubber on frost resistance of concrete and effect mechanism.* Procedia Engineering 2012;27:206-213.

[28] A. Richardson, K. Coventry, V. Edmondson, and E. Dias. *Crumb rubber used in concrete to provide freeze–thaw protection (optimal particle size).* Journal Of Cleaner Production 2016;112:599-606.

[29] A.E. Richardson, K. Coventry, and G. Ward. *Freeze/thaw protection of concrete with optimum rubber crumb content.* Journal Of Cleaner Production 2012;23(1):96-103.

[30] B. Savas, S. Ahmad, and D. Fedroff. *Freeze-thaw durability of concrete with ground waste tire rubber.* Transportation Research Record: Journal of the Transportation Research Board 1997;(1574):80-88.

[31] ASTM, *C666/C666M − 15: Standard Test Method for Resistance of Concrete to Rapid Freezing and Thawing*. 2015.

[32] A.J. Kardos and S.A. Durham. *Strength, durability, and environmental properties of concrete utilizing recycled tire particles for pavement applications.* Construction and Building Materials 2015;98:832-845.

[33] T.C. Powers and T. Willis. *The air requirement of frost resistant concrete*. in *Highway Research Board Proceedings*. 1950.

[34] T.C. Powers. *A working hypothesis for further studies of frost resistance of concrete*. in *Journal Proceedings*. 1945.

[35] D.H. Bager. *Qualitative description of the micro ice body freeze-thaw damage mechanism in concrete*. in *Workshop proceeding no. 9: Nordic miniseminar: Freeze-Thaw Testing of Concrete – Input to revision of cen test methods*. 2010.

[36] B. Johannesson. *Dimensional and ice content changes of hardened concrete at different freezing and thawing temperatures.* Cement and Concrete Composites 2010;32(1):73-83.

[37] A. Benazzouk, O. Douzane, T. Langlet, K. Mezreb, J. Roucoult, and M. Quéneudec. *Physico-mechanical properties and water absorption of cement composite containing shredded rubber wastes.* Cement and Concrete Composites 2007;29(10):732-740.

[38] A. Alsaif, L. Koutas, S.A. Bernal, M. Guadagnini, and K. Pilakoutas. *Mechanical performance of steel fibre reinforced rubberised concrete for flexible concrete pavements.* Construction and Building Materials 2018;172:533-543.

[39] BSI. *EN 13877-1. Concrete pavements Part 1: Materials. BSI 389 Chiswick High Road London W4 4AL UK.* 2013.

[40] A. Alsaif, S.A. Bernal, M. Guadagnini, and K. Pilakoutas. *Durability of steel fibre reinforced rubberised concrete exposed to chlorides.* Construction and Building Materials 2018;188:130-142.

[41] ASTM, *C136: Standard test method for sieve analysis of fine and coarse aggregates. ASTM International, West Conshohocken, PA. doi:10.1520/C0136-06.* 2006.

[42] H. Hu, P. Papastergiou, H. Angelakopoulos, M. Guadagnini, and K. Pilakoutas. *Mechanical properties of SFRC using blended manufactured and recycled tyre steel fibres.* Construction and Building Materials 2018;163:376-389.
[43] BSI, *BS 8500-1:2015+A1:2016.Concrete – Complementary British Standard to BS EN 206. Part 1: Method of specifying and guidance for the specifier.* 2016.
[44] BSI, *EN 12350-2: Testing fresh concrete, Part 2: Slump-test. BSI 389 Chiswick High Road, London W4 4AL, UK.* 2009.
[45] BSI, *EN 12350-7: Testing fresh concrete, Part 7: Air content — Pressure. BSI 389 Chiswick High Road, London, W4 4AL, UK.* 2009.
[46] BSI, *EN 12350-6: Testing fresh concrete Part 6: Density. BSI 389 Chiswick High Road, London, W4 4AL, UK.* 2009.
[47] BSI, *EN 12390-2: Testing hardened concrete, Part 2: Making and curing specimens for strength tests. BSI 389 Chiswick High Road, London W4 4AL, UK.* 2009.
[48] BSI, *PD CEN/TS 12390-9: Testing hardened concrete - Part 9: Freeze-thaw resistance with de-icing salts - Scaling. BSI 389 Chiswick High Road, London W4 4AL, UK.* 2016.
[49] BSI, *PD CEN/TR15177: Testing the freeze-thaw resistance of concrete - Internal structural damage. BSI 389 Chiswick High Road, London W4 4AL, UK.* 2006.
[50] BSI, *EN 12390-3: Testing hardened concrete, Part3: Compressive strength of test specimens. BSI 389 Chiswick High Road, London W4 4AL, UK.* 2009.
[51] JSCE. *SF-4: Method of test for flexural strength and flexural toughness of steel fiber reinforced concrete. Japan Concrete Institute, Tokio, Japan.* 1984.
[52] TI-B, *101. Test Method. Expansion Coefficient of Concrete. Danish Technological Institute Building Technology.* 1994.
[53] FDA, *Federal Highway Administration Research and Technology. Coordinating, Developing, and Delivering Highway Transportation Innovations*. 2016.
[54] T. Harrison, J.D. Dewar, and B. Brown, *Freeze-thaw Resisting Concrete: Its Achievement in the UK*. 2001: CIRIA.
[55] ASTM, *C672 / C672M-12: Standard Test Method for Scaling Resistance of Concrete Surfaces Exposed to Deicing Chemicals, ASTM International, West Conshohocken, PA,* www.astm.org. 2012.
[56] J. Yuan, Y. Liu, H. Li, and C. Yang. *Experimental investigation of the variation of concrete pores under the action of freeze-thaw cycles.* Procedia Engineering 2016;161:583-588.
[57] Swedish standards. *SS 13 72 44 ED. 4.Concrete Testing - Hardened Concrete - Scaling At Freezing. Standardiserings-Kommissionen I Sverige.* 2005.
[58] G. Skripkiūnas, A. Grinys, and E. Janavičius. *Porosity and durability of rubberized concrete*. in *The Second International Conference on Sustainable Construction Materials and Technologies*. 2010.
[59] K. Najim and M. Hall. *Mechanical and dynamic properties of self-compacting crumb rubber modified concrete.* Construction and Building. Materials. 2012;27(1):521-530.
[60] RILEM, *TC 176-IDC: Internal damage of concrete due to frost action, Final Recommendation, Prepared by L. Tang and P.-E. Petersson SP Swedish National Testing and Research Institute, Boras, Sweden. Materials and Structures / Mat6riaux et Constructions, Vol. 37,December 2004, pp 754-759* in *Slab test: Freeze/thaw resistance of concreteInternal deterioration* 2004.
[61] V. Baroghel-Bouny. *Evaluation and prediction of reinforced concrete durability by means of durability indicators. Part I: new performance-based approach*. in *ConcreteLife'06-International RILEM-JCI Seminar on Concrete Durability and Service Life Planning: Curing, Crack Control, Performance in Harsh Environments*. 2006: RILEM Publications SARL.
[62] M. Alexander, J. Mackechnie, and Y. Ballim. *Guide to the use of durability indexes for achieving durability in concrete structures.* Research monograph 1999;2.